EXCITATION OF FAST HYDROGEN ATOMS IN THE 2s, 2p AND 3p STATES DUE TO COLLISIONS WITH NOBLE GAS ATOMS

A. L. ORBELI, E. P. ANDREEV, V. A. ANKUDINOV, and V. M. DUKELSKIĬ

A. F. Ioffe Physico-technical Institute, USSR Academy of Sciences

Submitted February 7, 1969

Zh. Eksp. Teor. Fiz. 57, 108–116 (July, 1969)

Intensities of the L_α and L_β Lyman lines emitted in collisions between fast hydrogen atoms (5–40 keV) and He, Ne, Ar, Kr or Xe atoms are measured, and the cross sections for transition of hydrogen atoms to the 2s, 2p or 3p states are determined. In the energy range studied the cross sections $\sigma(2p)$ and $\sigma(2s)$ are of the order of 10^{-17} cm^2, whereas $\sigma(2p) > \sigma(2s)$; the cross section $\sigma(3p)$ is of the order of 10^{-18} cm^2. Cross sections $\sigma(2p)$ and $\sigma(3p)$ for He and $\sigma(2s)$ and $\sigma(2p)$ for Ne decrease monotonously with increase of energy. The $\sigma(2p)$ curves for Ar, Kr and Xe and the $\sigma(3p)$ curve for Kr have two maxima. The cross sections for the $H(1s) + He(1s^2) \rightarrow H(2p, 3p) + He(1s^2)$ processes calculated in the first Born approximation decrease with increase of energy in agreement with the experiments.

1. INTRODUCTION

SEVERAL recent experimental papers are devoted to measurements of the cross sections for the capture of electrons by protons (on passing through gases) with production of hydrogen atoms in excited states with n = 2 and n = 3[1-8]. Practically no investigations have been made to date of the direct excitation of fast hydrogen atoms in collisions with gas atoms[7,9], although this process seems to be simpler, since it can occur without a change of the state of the gas atom.

In this article we report measurements of the intensity of the first two lines of the Lyman spectrum L_α (λ = 1216 Å) and L_β (λ = 1026 Å), excited by collisions between fast hydrogen atoms (energy 5–40 keV) and He, Ne, Ar, Kr, or Xe atoms. The intensity of the L_α line yielded the cross sections for the excitation of hydrogen atoms in the 2p state. The cross sections for the excitation of the 2s state were determined by measuring the increase of the intensity of the line L_α when an electric field is produced in the collision region. Data on the intensity of the L_β line have made it possible to calculate the cross sections for the excitation of the 3p state.

2. APPARATUS, MEASUREMENT METHOD

We used a setup which was previously employed to study the excitation of the L_α and L_β lines in the capture of an electron by protons[1,5]. To obtain a beam of fast hydrogen atoms, an additional chamber was introduced into this setup, in which the proton beam was partly neutralized by capture of electrons in the gas.

The experimental setup is shown in Fig. 1. A monokinetic proton beam[1)] was guided by means of a quadrupole doublet 4 into the neutralization chamber 5, filled with neon to a pressure 10^{-2} mm Hg. A parallel-plate capacitor 6 was used to deflect the charged particles, and also to convert the 2s-state metastable hydrogen atoms produced in the neutralization chamber into the 2p state. The neutral beam then passed through slit 7 into the collision chamber, into which the various inert gases could be admitted. After passing through the collision chamber, the fast-particle flux was measured with a thermoelectric detector 12[10] calibrated with the aid

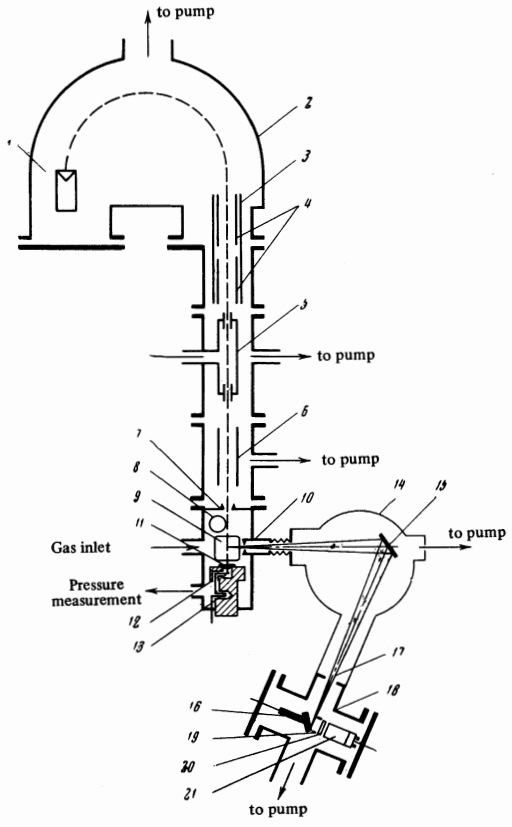

FIG. 1. Experimental setup: 1–ion source, 2–vacuum chamber of mass spectrometer, 3–magnetic screen, 4–quadrupole doublet, 5–neutralization chamber, 6–parallel-plate capacitor, 7–input slit of collision chamber (3 × 8 mm), 8–nitrogen trap, 9–parallel-plate capacitor, 10, 17–input and output slits of vacuum monochromator, 11–"hot" junction of thermal detector (copper foil–constantan), 12–copper body of thermal detector, 13–"cold" junction of thermal detector, 14–vacuum monochromator, 15–diffraction grating, 16–photoelectronic converter, 18–vacuum chamber of quantum counter, 19–focusing electrode, 20–scintillator, 21–photoelectronic multiplier (FÉU-38)

of a proton beam. In the energy interval from 5 to 40 keV, the equivalent current of neutral atoms of hydrogen ranged from 2 to 40 μA. A parallel-plate capacitor 9 was placed in the collision chamber and made it possible to produce an electric field perpendicular to the plane of the figure. The light produced by the passage of the beam of fast hydrogen atoms through the gas in the collision chamber was observed at an angle of 90° to the direction of the beam and was analyzed with a vacuum monochromator 14 of the Seija-Namioka type. Detection and the measurements of the intensity of the spectral lines was by means of a photoelectric quantum counter 18.

The method used to measure the intensities of the lines L_α and L_β was the same as that used in the study of the excitation of these lines during the process of electron capture by protons[1,5]. A quantum counter was used to perform relative measurements of the intensities of the lines L_α and L_β in the indicated range of energies of the fast hydrogen atoms for all the inert gases. During the course of observation of the L_α line, two measurements were made at each point: 1) in the absence of an electric field in the collision chamber, when the count was proportional to the cross section $\sigma(2p)$ for the excitation of the excited 2p state, and 2) when an electric field of intensity 600–800 V/cm was applied to transfer the hydrogen atoms from the metastable 2s state to the 2p state, when the count was proportional to the sum of the cross sections $\sigma(2p) + \sigma(2s)$. The ratio $\sigma(2s)/\sigma(2p)$ was determined from these two counts.

The absolute values of the cross sections $\sigma(2p)$ were determined by comparing the intensity of the line L_α produced by excitation of the beam of fast hydrogen atoms with the intensity of the same line excited by passage of a proton beam through the collision chamber. The absolute cross sections $\sigma(2p)$ of the second process were determined earlier in[1]. The absolute values of the cross sections for the excitation of fast hydrogen atoms in the 3p state were determined from measurements of the intensity of the L_β line in the absence of an electric field, by comparison with the intensity of this line as excited in the process of electron capture by protons[5]. In measurements of the intensity of the line L_β, account was taken of the correction for the lifetime of the 3p state. For greater reliability and to verify the obtained data, relative measurements were made also of the intensities of the lines L_α and L_β for all gases during one and the same experiment, at two or three values of the hydrogen-atom beam energy.

In all the direct measurements of the L_α and L_β line intensities, usual control experiments were performed. The dependence of the measured intensity on the gas density in the collision chamber and on the flux of the fast hydrogen atoms was determined. The main measurements were performed at gas pressures $(3-7) \times 10^{-4}$ mm Hg. Measurements of the effect alternated with measurements of the background at a residual pressure of 2×10^{-5} mm Hg in the collision chamber.

3. RESULTS

For lack of space, we do not present here data on the excitation cross sections of the lines L_α and L_β in the absence and in the presence of an electric field in the collision chamber. Some of the results on the excitation of L_α were reported at the fifth international conference on the physics of electronic and atomic collisions (Leningrad, 1967) and were published in the abstract collection[11]. Figure 2 shows the cross sections for the transition of the fast hydrogen atoms into the states 2s, 2p, and 3p by collision with He, Ne, Ar, Kr, and Xe atoms.

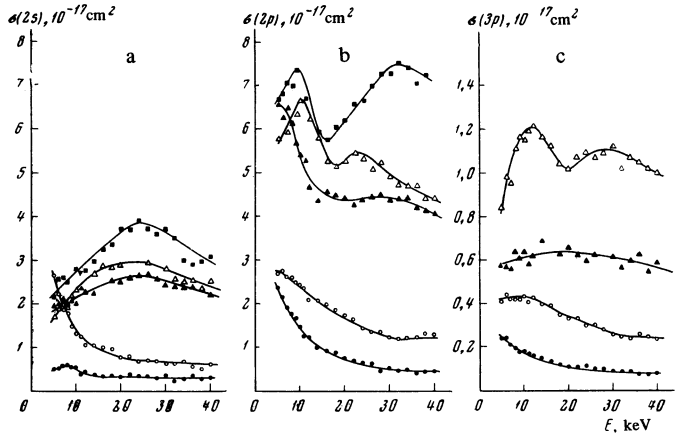

FIG. 2. Energy dependence of the excitation cross sections of hydrogen atoms in the states 2s, 2p, and 3p in collisions with atoms of He (●), Ne (○), Ar (▲), Kr (△), and Xe (■).

The accuracy of the curves of Fig. 2 is determined by the statistical error of the relative measurements of the intensities of the lines L_α and L_β. This error amounted on the average to ±10%. The error introduced in the relative position of the curves in each of the figures 2a, b, c is somewhat larger, up to ±15%. The correctness of the relative position of the curves for the cross sections $\sigma(2p)$ and $\sigma(2s)$ depends on the error in the measurement of the intensity of the line L_α in the absence of an electric field and with the electric field applied. This error amounted, on the average, also to ±15%.

The absolute values of the cross sections, given by the curves of Fig. 2, were determined with a much higher error. Besides the error in the relative measurements of the intensities of the lines L_α and L_β, it contains the errors in the determination of the absolute cross sections for the excitation of the states 2p and 3p in the case of electron capture by a proton. The value $\sigma(2p) = 8.9 \times 10^{-18}$ cm^2 for the process $H^+ + Ne \rightarrow H(2p) + Ne^+$ is given in[1] with an error of ±20%. For other inert gases, the errors in the cross sections, indicated in this article, can be larger, up to ±25%. Thus, the maximum mean-squared errors of the absolute values of the cross sections $\sigma(2p)$ (Fig. 2b) can reach ±30%. The errors in the cross sections $\sigma(2s)$ (Fig. 2a) and $\sigma(3p)$ (Fig. 2c) are ±35% and ±40%, respectively.

An analysis of the errors suggests that the peculiarities of the curves of Fig. 2 should be approached with caution. The statements that follow apparently do not depend on the limited accuracy of our results.

1. In the fast hydrogen-atom energy interval 5–40 keV, the cross sections for the excitation of the levels 2p and 3p in the case of He, and of the levels 2p,

2s, and 3p in the case of Ne, decrease with increasing energy.

2. In the case of Ar, Kr, and Xe the cross sections $\sigma(2s)$ reach a maximum at an energy 20—30 keV. The curves for the cross sections $\sigma(2p)$ have two maxima: at 10 and at 20—30 keV.

3. All the cross sections increase on going over from the lighter atom of the target to the heavier one.

4. In all gases, with the exception of Ne, the cross sections $\sigma(2p)$ are larger than the cross sections $\sigma(2s)$ by a factor 2—3; in Ne, at an energy of approximately 5 keV, these cross sections turn out to be close in magnitude. The cross section $\sigma(3p)$ is smaller than the cross section $\sigma(2p)$ for the same gas by a factor 5—10.

More subtle features of the curves of Fig. 2, for example the weakly pronounced maximum for the cross section $\sigma(2s)$ in He at $E \approx 8$ keV, the increase of the cross section $\sigma(2p)$ in Ne at $E > 30$ keV, the strong scatter of the points for the cross section $\sigma(3p)$ in Ar, all lie within the limits of errors.

4. DISCUSSION OF RESULTS

We found no published theoretical papers dealing with the process investigated by us, the excitation of hydrogen atoms by collision with inert-gas atoms. We are therefore forced, in discussing our results, to confine ourselves to qualitative considerations regarding the observed energy dependences of the cross sections of this process.

We note that in our experiments the emission of the lines L_α and L_β was due to direct excitation of hydrogen atoms in the 1s state only. Of course, the beam of neutral hydrogen atoms produced in the neutralization chamber should contain a certain fraction of excited atoms. But in the field of the capacitor 6 (Fig. 1), practically all the atoms in the 2s state should go over to the 2p state, and should then emit on the path from the capacitor 6 to the collision chamber. The hydrogen atoms in the state with principal quantum number n = 3 could likewise not reach the collision chamber, since the average lifetime of this state is small compared with the time of flight to the collision chamber. As to the excited states with $n > 3$, the average lifetimes of which are comparable with the time of flight, they could not constitute an appreciable admixture to the hydrogen atoms in the ground state, owing to the small probability of their excitation upon neutralization of the protons.

It can be further assumed that an inert-gas atom remains after collision in the same ground state as prior to the collision. This assumption is based on the fact that simultaneous excitation of both particles calls for a much higher energy than the excitation of one particle. The energy required to excite the 2s or 2p level of the hydrogen atom is 10.2 eV, and the energy required for simultaneous excitation of one of these levels and of the level $1s2p\,^1P_1$ of the He atom is 31.3 eV. In the case of Ne, simultaneous excitation of both particles requires an energy not less than 26.8 eV. For the heavy gases Kr and Xe, it apparently cannot be assumed that the process of simultaneous excitation of both partners of the collision, in the entire investigated energy range, has just as low a probability as in the case of He and Ne (see below).

Some small contribution to the measured cross sections might come from cascade transitions from higher excited states of the hydrogen atom[11]. In the present investigation, the influence of cascade transitions was not taken into account. The small anisotropy of the spatial distribution of the radiation L_α [12] and L_β was likewise neglected.

Let us examine the properties, listed by us in section 3, of the excitation curves obtained by us.

1. The decrease of the cross sections $\sigma(2s)$, $\sigma(2p)$, and $\sigma(3p)$ in the energy interval 5—40 keV in the case of collision of hydrogen atoms with He and Ne atoms is somewhat unexpected. For inelastic collision with an energy loss 10.2 eV (2s, 2p) or 12.1 eV (3p) in this energy interval, one should expect the cross sections to increase or to have a maximum, just as in the case of the excitation of the 2s state of Ar, Kr, or Xe (Fig. 2a) or in the case of electron loss by fast hydrogen atoms in inert gases[13,14]. It is seen from Fig. 2 that the maxima for the cross sections $\sigma(2p)$ and $\sigma(3p)$ in the case of He, and also for the cross sections $\sigma(2s)$ and $\sigma(2p)$ in the case of Ne, lie at an energy lower than 5 keV. In the case of He, a decrease of the curve towards lower energies is observed for the cross section $\sigma(2s)$, starting with 7 keV. The sum of the cross sections $\sigma(2s) + \sigma(2p)$ at 5 keV is $\sim 3 \times 10^{-17}$ cm^2 in the case of He and $\sim 5 \times 10^{-17}$ cm^2 in the case of Ne. The maxima at an energy lower than 5 keV, and also the large cross sections at hydrogen-atom velocities much lower than the Bohr velocity $e^2/\hbar$, give grounds for assuming that the energy necessary for the system $H(1s)He(1s^2)$ to go over to the excited states $H(2s, 2p, 3p)He(1s^2)$ decreases appreciably when the distance between the atoms H and He is of the order of the Bohr radius of the hydrogen atom.

One of the present authors (V. A. A.) calculated the cross sections for the processes

$$H(1s) + He(1s^2) \to H(2s, 2p, 3p) + He(1s^2).$$

The cross sections for the excitation of the hydrogen atoms in the states 2s, 2p, and 3p were calculated in the first Born approximation without allowance for the exchange effects. The wave function of the ground state of the helium atom was chosen to be a variational-single-parameter function. Following[15,17], for example, it is easy to obtain an expression for the cross section of the simple transition, in which a fast hydrogen atom is excited in the state nl, and the He atom does not change its state:

$$\sigma(1s-nl;\ 1s^2-1s^2) = \frac{32\pi a_0^2}{s^2}\int_{t_{min}}^{t_{max}}\left[1-\frac{16\alpha^4}{(4\alpha^2+t^2)^2}\right]^2 |J(1s-nl)|^2\frac{dt}{t^3},$$

where $\alpha = 27/16$, a_0 is the radius of the first Bohr orbit, $s = v/v_i$, v_i is the electron velocity on this orbit, v is the velocity of the incoming hydrogen atom,

$$J(1s-nl) = \int \chi_{1s}^{*}(\rho)\,\chi_{nl}(\rho)\,e^{-it\rho}\,d^3\rho,$$

and $\chi(\rho)$ are the wave functions of the hydrogen atom. For the transitions investigated by us (see[15] or[17])

$$|J(1s-2s)|^2 = \frac{2^{17}t^4}{(4t^2+9)^6},$$

$$|J(1s-2p)|^2 = \frac{2^{15}\cdot 3^2 t^2}{(4t^2+9)^5},$$

$$|J(1s-3p)|^2=\frac{2^{11}\cdot 3^6 t^2(27t^2+16)^2}{(9t^2+16)^8}$$

At not too low energies of the incoming hydrogen atom we have

$$t_{min}\approx\frac{\Delta E(1s-nl)}{2s},\quad t_{max}=\infty,$$

where $\Delta E(1s-nl)$ is the transition energy in units of the ionization potential of the hydrogen atom.

The cross sections were calculated by numerical integration. Although the approximation is valid at energies higher than 25 keV, we have calculated, for comparison with experiment, the cross sections also for lower energies of the hydrogen atom. It is seen from Fig. 3 that the variation of the experimental and theoretical cross sections with energy, for the transitions 1s–2p and 1s–3p, is approximately the same. As to the satisfactory agreement between the absolute values, it should be regarded as accidental, first because the approximation itself is very crude in the investigated energy interval, and second because the energy needed for the transition may turn out to be much lower when the colliding atoms come close together, than the energy at infinity. In the latter case, the theoretical curves will lie much higher than those shown in Fig. 3.

2. The dependence of the cross sections $\sigma(2s)$ on the energy in the case of Ar, Kr, and Xe differs greatly from the dependence in the case of He and Ne. The curves for Ar, Kr, and Xe have a "normal" form, with one maximum in the investigated energy interval. The cross section increases at the maximum in the sequence Ar → Kr → Xe.

The plots of the cross sections $\sigma(2p)$ for Ar, Kr, and Xe have two maxima, unlike the plots for the cross sections $\sigma(2s)$. The causes of the second maximum of $\sigma(2p)$ at higher energies can only be conjectured. It is most natural to assume that the first maximum pertains to the process of excitation of fast hydrogen atoms without a change in the state of the inert-gas atom, while the second maximum corresponds to the process of simultaneous excitation of both colliding particles; nor is ionization of the target atom excluded. Under this assumption, it still remains unclear why the curves for the cross sections $\sigma(2s)$ have only a single maximum.

A curve with two maxima was obtained also for the cross section $\sigma(3p)$ in the case of Kr (Fig. 2c); this curve can be interpreted in the same manner as the curve for the cross section $\sigma(2p)$.

3. The increase of the cross sections on going from the lighter inert-gas atom to the heavier one is a normal phenomenon for all inelastic collisions of atomic particles. The intersection of the plots of $\sigma(2s)$ in the energy region near 5 keV is due to the "anomalous" course of the curve for Ne.

4. It can be expected that the course of the curves for the cross sections $\sigma(3p)$ will be similar to the course of the corresponding curves for the cross section $\sigma(3p)$. However, there is no complete similarity between the curves for $\sigma(3p)$ and $\sigma(2p)$. Nonetheless, owing to the large errors in the measurements of the cross sections $\sigma(3p)$ and $\sigma(2p)$, one cannot insist that the observed deviations are real.

The cross sections obtained in the present paper for the process of direct excitation of hydrogen atoms can be compared with the cross sections for the excitation of the same states during the process of electron capture by protons[1,5]. Figure 4a shows the plots for these two processes in the case of collisions with He atoms. At energies lower than 20 keV, the forms of the curves for these two processes are different: the cross sections for the direct-excitation process exceed the cross sections for the electron capture by the protons. This difference can be attributed to the fact that in the case of electron capture by protons the energy loss is higher than in the case of direct excitation, by the amount of energy necessary to transfer the electron from the gas atom to the ground level of the hydrogen atom. In the case of He, this additional energy loss is equal to 11 eV. At energies larger than 30 keV, the difference becomes smoothed out. The cross section $\sigma(2s)$ for the capture of an electron by protons becomes even larger than for the process of direct excitation of the hydrogen atoms.

In Fig. 4b, the cross sections of the two processes are compared for the heavier atom Kr. In this case, the energy lost in the capture of the electron by the proton

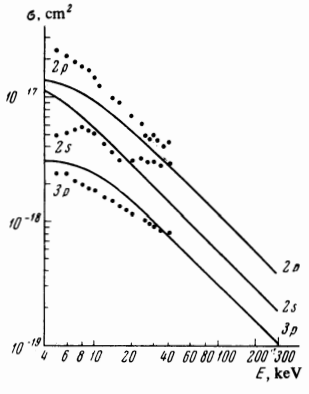

FIG. 3. Comparison of experimental cross sections for the excitation of hydrogen atoms in the states 2s, 2p, and 3p in He (points) with those calculated in the first Born approximation (solid lines). When $E > 300$ keV, $\sigma(2s) \sim 0.65\, E^{-1}\pi a_0^2$, $\sigma(2p) \sim 1.27\, E^{-1}\pi a_0^2$, and $\sigma(3p) \sim 0.36\, E^{-1}\pi a_0^2$, where E is in keV.

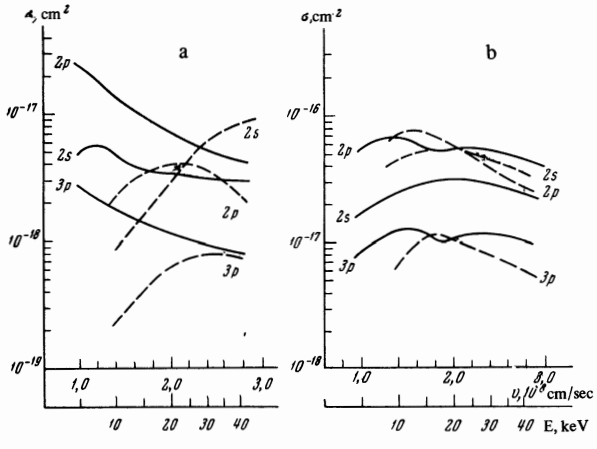

FIG. 4. Comparison of the cross sections for the excitation of hydrogen atoms in the states 2s, 2p, and 3p (solid lines) with the excitation cross sections of the same states in the capture of an electron by protons (dashed lines) in the case of He (a) and in the case of Kr (b).

at the ground level of the hydrogen atom is only 0.4 eV, i.e., it is small compared with the excitation energies of the states 2s, 2p, and 3p of the hydrogen atom, so that the energies lost in the two processes are practically equal. In the case of Kr, there are likewise no significant differences between the excitation curves of the two processes. However, for Kr, just as for Ar and Xe, the differences between the cross sections of the two compared processes exceed the measurement errors. These differences are connected apparently not only with the magnitude of the energy loss, but also with the peculiarities of both excitation processes.

[1] E. P. Andreev, V. A. Ankudinov, and S. V. Bobashev, Zh. Eksp. Teor. Fiz. 50, 565 (1966) [Sov. Phys.-JETP 23, 375 (1966)].

[2] D. Jaecks, B. van Zyl, and R. Geballe, Phys. Rev. 137, A340 (1965).

[3] E. P. Andreev, V. A. Ankudinov, and S. V. Bobashev, V ICPEAC, 1967, Abstracts of papers, pp. 307, 309.

[4] B. van Zyl, D. Jaecks, D. Pretzer, and R. Geballe, Phys. Rev. 158, 29 (1967).

[5] E. P. Andreev, V. A. Ankudinov, S. V. Bobashev, and V. B. Matveev, Zh. Eksp. Teor. Fiz. 52, 357 (1967) [Sov. Phys.-JETP 25, 232 (1967)].

[6] R. H. Hughes, H. R. Dawson, B. M. Doughty, D. B. Kay, and C. A. Stigers, Phys. Rev. 146, 53 (1966).

[7] D. A. Dahlberg, D. K. Anderson, and I. E. Dayton, Phys. Rev. 164, 20 (1967); 170, 127 (1968).

[8] J. E. Bayfield, Phys. Rev. Lett. 20, 1223 (1968).

[9] V. Dose, R. Gunz, and V. Meyer, Helv. Phys. Acta 41, 269 (1968).

[10] R. Cardon, Rev. Sci. Instr. 24, 366 (1953).

[11] V. A. Ankudinov, E. P. Andreev, and A. L. Orbeli, V ICPEAC, 1967, Abstracts of papers, p. 312.

[12] V. Dose, R. Gunz, and V. Meyer, Helv. Phys. Acta 41, 264 (1968).

[13] P. M. Stier and C. F. Barnett, Phys. Rev. 103, 896 (1956).

[14] Ya. M. Fogel', V. A. Ankudinov, D. V. Pilipenko, and N. V. Topolya, Zh. Eksp. Teor. Fiz. 34, 579 (1958) [Sov. Phys.-JETP 7, 400 (1958)].

[15] D. R. Bates and G. W. Griffing, Proc. Phys. Soc. A66, 961 (1953).

[16] D. R. Bates and A. Williams, Proc. Phys. Soc. A70, 306 (1957).

[17] Atomic and Molecular Processes, ed. by D. R. Bates, Academic Press, 1962, ch. 14.

Translated by J. G. Adashko
14

REDUCED ABSORPTION OF THE Nd^{3+} *ION IN VARIOUS BASES*

Yu. K. VORON'KO, M. V. DMITRUK, G. V. MAKSIMOVA, V. V. OSIKO, M. I. TIMOSHECHKIN, and I. A. SHCHERBAKOV

P. N. Lebedev Physics Institute, U.S.S.R. Academy of Sciences

Submitted February 11, 1969

Zh. Eksp. Teor. Fiz. 57, 117–124 (July, 1969)

The integral absorption of a single Nd^{3+} ion is investigated in various matrices and at various concentrations. Comparison of the experimental data and theory yield information on the statistics of the optical centers and their symmetry.

INTRODUCTION

INTEGRAL absorption of rare-earth ions introduced in a crystal base is not only an important characteristic influencing laser output parameters, but also a quantity capable of yielding important information regarding the processes occurring in activated crystals. It is well known qualitatively that the values of the integral absorption of equal concentrations of the same ion introduced into different hosts are essentially different. In addition, on the basis of the results of one of our earlier investigations,[1] we can expect the integral absorption per ion to depend in some cases on the activator concentration. In the present investigation we studied the relative absorption of the Nd^{3+} ion in a large number of hosts having different crystal structures and optical-center structures. In most hosts, the Nd^{3+} concentration was varied in a wide range.

INVESTIGATED CRYSTALS AND EXPERIMENTAL PROCEDURE

The table lists a summary of the investigated hosts in which the Nd^{3+} ion was introduced, and some of their characteristics.[1-3] All the crystals were grown in accordance with the procedures described in [4,5,10,11] The divalent fluorides were crystals of type I (see [12]). The investigated characteristic was chosen to be the relative absorption

$$J=\frac{1}{n_0}\int_{\Delta\nu} k(\nu)\,d\nu, \qquad (1)$$

where n_0 is the number of Nd^{3+} ions per cm^3, $k(\nu)$ is the absorption coefficient of light of frequency ν (in cm^{-1}), and $\int_{\Delta} k(\nu)d\nu$ is (in the case of Nd^{3+}) the absorption due to the transitions, in the interval $\Delta\nu$, from the Stark components of the ground level $^4I_{9/2}$, populated at room temperature, to the Stark components of the excited levels $^4F_{3/2}$; $^4F_{5/2}$, $^2H_{9/2}$; $^4F_{7/2}$, $^4S_{3/2}$; $^2G_{7/2}$, $^4G_{5/2}$. The absorption was measured in these groups because these are precisely the transitions that make the main contribution to the integral absorption of laser crystals activated with Nd^{3+}.

Absorption spectra in the form $1-I/I_0=f(\lambda)$ (where I_0 is the intensity of the incident light and I the intensity of the transmitted light) were obtained at room temperature with an SF-8 spectrophotometer using a

Host	Nd^{3+} concentration, wt.%	Lattice structure* [2,4,5]	Lines in absorption spectra**	τ_{rad} of the Nd^{3+} ion level, msec [1,2,5,6,7]
CaF_2	0.1—5	cub, O_h^5-Fm3m	L, $(M+N)$, P[8]	$\begin{cases}L-1.2\\M+N->0.1\end{cases}$
SrF_2	0.1—5	cub, O_h^5-Fm3m	L, M, P [1]	$\begin{cases}L-1.2\\P-0.12\end{cases}$
BaF_2	0.3—10	cub, O_h^5-Fm3m	L, M, P [1]	$\begin{cases}L-8\\P-0.26\end{cases}$
LaF_3	0.1—4	hex, D_{6h}^3-C6/mcm	OTC [7]	0.7—0.08
CeF_3	0.3—4	hex, D_{6h}^3-C6/mcm	OTC [5]	0.3—0.18
CaF_2-YF_3(3 wt.%)	0.1—4	cub, O_h^5-Fm3m	MC [8]	1—0.7
CaF_2-YF_3(6 wt.%)	0.1—4	cub, O_h^5-Fm3m	MC [8]	1—0.7
CaF_2-YF_3(12 wt.%)	0.1—4	cub, O_h^5-Fm3m	MC [8]	1—0.7
CaF_2-CeF_3(3 wt.%)	0.3—1	cub, O_h^5-Fm3m	MC [8]	0.7
CaF_2-CeF_3(5 wt.%)	0.3—1	cub, O_h^5-Fm3m	MC [8]	0.7
BaF_2-LaF_3(30 wt.%)	1—8	cub, O_h^5-Fm3m	MC [8]	0.8
$Y_3Al_5O_{12}$	0.3	cub, $O_h(10)-Ia3d$	STC [9]	0.2
Silicate glass	3.6	—	MC	0.4
$CaWO_4-Nb$	0.05—1.5	tetr., C_{4h}^6-I4/a	STC [9]	0.175
$CaWO_4-Na$	0.05—1.5	tetr., C_{4h}^6-I4/a	STC [9]	0.175

*Notation: cub. – cubic lattice, hex. – hexagonal lattice, tetr – tetragonal lattice.

**Notation: OTC – one type of center, MC – multiplicity of centers, STC – several types of centers.